

## Alkali cations enhance Zr-beta zeolite selectivity in citronellal Meerwein-Ponndorf-Verley reduction

Jan Přečh\*, Jun Xie, Mariya Shamzhy, Jiří Čejka\*

Department of Physical and Macromolecular Chemistry, Faculty of Science, Charles University, Albertov 6, 128 43 Prague 2, Czech Republic

\*Corresponding author: [jan.prech@natur.cuni.cz](mailto:jan.prech@natur.cuni.cz), phone: +420 221 95 1322 (J.P.),  
[jiri.cejka@natur.cuni.cz](mailto:jiri.cejka@natur.cuni.cz), phone: +420 221 95 1032 (J.C.)

### Abstract

Zr-silicate zeolites efficiently catalyze Meerwein-Ponndorf-Verley (MPV) reduction, a key reaction in fine chemical production. However, for substrates such as citronellal, MPV reaction selectivity decreases due to competing Lewis acid-catalyzed reactions, notably carbonyl-ene cyclization, which yields isopulegol as the main product. Reaction selectivity may be determined by site strength as weaker “closed” sites in Zr-beta catalyze MPV reduction, while stronger “open” Zr sites catalyze carbonyl-ene cyclization. But the precise control over acidity strength in Zr-beta catalysts remains an unsolved challenge. This study aims at modulating Al-free Zr-beta zeolite acidity through ion exchange with Li<sup>+</sup>, Na<sup>+</sup> and Cs<sup>+</sup> ions. In citronellal MPV reduction, we increased citronellol selectivity by tuning the Lewis acidity of Zr-beta. As shown by FT-IR spectroscopy of acetone and d<sub>3</sub>-acetonitrile, ion exchange weakened interactions between carbonyl compounds and “open” Zr Lewis acid sites, converting strong Zr “open” sites into weaker Lewis acid sites and, thus, switching the reaction selectivity from the isopulegol to the MPV reduction. Case in point, ion-exchanged Zr-beta-1-Na<sup>+</sup>4x provided 77% citronellol selectivity and 23% isopulegol selectivity. In contrast, non-exchanged Zr-beta-1 afforded 26% citronellol selectivity and 73% isopulegol selectivity, at a similar conversion level, without significant changes in the overall rate of citronellal conversion. These findings highlight ion exchange as an effective tool for post-synthesis control of Zr-beta Lewis acidity.

**Keywords:** MPV reduction, Lewis acidity, Zr-zeolite, ion exchange, alkali cation, citronellal, citronellol, isopulegol

### 1. Introduction

Zeolites are microporous crystalline silicate materials with three-dimensional framework structure, formed by corner-sharing [TO<sub>4</sub>] tetrahedral units (T= Si, Al, Zr, Sn, Ti, and others)[1-4]. In the silicate zeolite framework, different tetravalent metals (such as Zr, Ti, Sn, Hf [5-7]) act as Lewis acids, which can accept electron pairs thanks to their empty d-orbitals [8-10]. Distributed as single atoms in silicate frameworks, these metal centers can catalyze oxidation reactions, such as epoxidation (Ti-silicates)[11] and Baeyer–Villiger Oxidation (Sn-silicates)[5, 12], carbonyl-ene reactions (Zr-, Sn-, and Hf-silicates)[13], and dehydration reactions (Zr-, Sn-, and Hf-silicates)[10, 14] and hydrogen transfer and rearrangement reactions, including the Meerwein–Ponndorf–Verley (MPV) reduction (Zr-, Sn-, and Hf-silicates)[15].

Through MPV reduction, ketones and aldehydes can be easily converted into their corresponding alcohols in the presence of other reducible groups, such as unsaturated C=C bonds[16, 17]. The MPV reaction proceeds via a cyclic six-membered transition-state complex in which both the carbonyl group and the alcohol are coordinated to the Lewis acid center, enabling a concerted hydride transfer from the alcohol to the carbonyl group [4, 18, 19]. Usually occurring at temperatures below 100 °C, MPV reduction uses secondary alcohols as hydrogen donors instead of molecular hydrogen, which simplifies the reaction setup.

For this reason, MPV reduction is particularly useful for synthesizing biomass-derived alcohols, many of which are important intermediates in the production of pharmaceuticals[19-22]. In some perfumes, both citronellal (3,7-dimethyl-6-octenal), a non-conjugated unsaturated aldehyde, and citronellol (3,7-dimethyl-6-octene-1-ol), its MPV reduction product, are essential components [23, 24].

In MPV reduction, the most commonly used zeolite catalysts are Zr- and Sn-substituted zeolites [9, 19, 25, 26]. The former show higher activity in aldehyde reduction, while the latter favor ketone reduction [9, 18, 27, 28]. However, researchers often overlook Zr-zeolites, primarily focusing on Sn-zeolites. For example, a search in the Web of Science Core Collection for the keyword “Zr-beta” in 2025 provides only 157 results, in contrast to 686 results for “Sn-beta”. The lack of studies on Zr-zeolites limits our ability to fully leverage their catalytic potential. In addition to framework-incorporated Zr atoms, these zeolites may also contain oxidic and oxide-like polyatomic species with properties similar to those of  $\text{ZrO}_2$  [10], but they are mostly catalytically inactive below 100 °C [29].

Zr-beta zeolites contain two main types of framework Zr Lewis acid sites, namely “closed”  $[\text{Zr}(\text{OSi})_4]$  and “open”  $[\text{Zr}(\text{OSi})_3\text{OH}]$  sites. Zr “open” sites are considered stronger Lewis acids than Zr “closed” sites [30-33]. The relationship between Lewis acidity and catalytic activity and selectivity has been studied because the MPV reduction of aldehydes over beta zeolites is typically accompanied by parallel reactions, including etherification [16], acetalization[9] and carbonyl-ene cyclization [13, 34]. Lewis acid sites are the active centers of Zr-zeolite beta in the MPV reduction of  $\alpha$ ,  $\beta$ -unsaturated aldehydes, as in the reduction of cinnamaldehyde to cinnamyl alcohol (> 98%) [16]. In contrast, Brønsted acid sites catalyze undesired cross-etherification of cinnamyl alcohol and 2-propanol, so Al-containing Zr-zeolite beta is less active and selective. Weak Lewis acid sites promote the MPV reduction of 4'-methoxypropiofenone, while stronger acid sites, presumably “open” Zr sites, catalyze the subsequent dehydration [35]. Increasing the concentration of Lewis acid sites in Zr-beta catalysts could significantly enhance their activity in the MPV reduction of cyclohexanone [36]. Thus, acid site strength is a key selectivity determinant.

In a recent study[29], we have shown that the type of Zr Lewis site determines the product selectivity of citronellal MPV reduction over Zr-beta. The weaker “closed” sites catalyze citronellal MPV reduction to citronellol, while the stronger “open” sites catalyze intramolecular carbonyl-ene cyclization to isopulegol. To achieve high selectivity in MPV reduction, we must therefore develop methods for regulating the Lewis acid site strength of Zr-beta zeolite. The most straightforward approach would be tailored synthesis of a material containing purely “closed” sites. However, this approach remains an unsolved synthetic challenge. Nevertheless, we can also regulate the Lewis acidic properties of zeolites by ion exchange with alkali metal cations.

For aluminosilicates, ion exchange of their Brønsted acid sites with alkali cations typically leads to the formation of weak Lewis acid sites. Lewis acidity is provided by empty orbitals of the cations. In the MPV reduction of citronellal over  $\text{Cs}^+$  ion-exchanged X-type (aluminosilicate FAU) zeolite, Cs-FAU, citronellol selectivity reaches 92.3% at 150 °C, while over Li-FAU and Na-FAU, isopulegol is formed instead, with 87.7 and 86% selectivity, respectively, as the reaction pathway is likely driven by steric effects related to the effective pore sizes of the ion-exchanged zeolites [37]. In turn, the catalytic activity of aluminosilicate H-beta zeolite in MPV reduction has been assigned to extra-framework  $\text{AlO}_x$  counter cations at ion-exchangeable sites that act as Lewis acids [23]. These sites catalyzed MPV reduction of 4-tert-butyl cyclohexanone with 2-propanol at a turn-over-frequency (TOF) of  $5150 \text{ h}^{-1}$  at 80 °C.

In Sn-beta, even OH groups of “open” Sn sites, whose Brønsted acidity is rather weak [10], can be ion-exchanged with Na<sup>+</sup>, shifting the reaction selectivity from glucose-fructose isomerization towards glucose epimerization to mannose [38]. Modifying Sn-beta with a small amount of cations (Li<sup>+</sup>, Na<sup>+</sup> and NH<sub>4</sub><sup>+</sup>) can passivate the Brønsted acidity of silanol groups adjacent to Sn atoms without changing the Lewis acidity, thereby improving caprolactone selectivity in the Baeyer–Villiger oxidation of cyclohexanone [39]. In Zr-Al-beta, Al Brønsted acid sites have been transformed into weak Lewis acid sites to promote MPV reduction of furfural to furfural alcohol by introducing alkali metal cations by ion exchange [40]. Beyond the deactivation of Brønsted sites, the acidity of Zr “open” Lewis sites was also weakened by introducing alkali-metal ions to Zr-Al-beta, which partly decreases the electropositivity of Zr atoms [40]. In line with this weakening of Zr Lewis acidity, we have also recently shown that ion exchange of “open” sites with Na<sup>+</sup> suppresses the carbonyl-ene cyclization of citronellal through site deactivation and accelerates its MPV reduction to some extent [29]. This effect suggests that the catalytic properties of at least some of the sites are modified in a way that favors MPV reduction over carbonyl-ene cyclization. Based on these findings, adjusting site acidity through modifications with appropriate alkali metal cations may improve the catalytic performance of Zr-beta, even in reactions where MPV reduction competes with other Lewis acid-catalyzed reactions.

Herein, we systematically characterize and investigate the catalytic properties of aluminum-free Zr-beta catalysts in their original state and after Li<sup>+</sup>, Na<sup>+</sup>, Cs<sup>+</sup> ion exchange in the competing MPV reduction/carbonyl-ene cyclization of citronellal. The type and concentration of Lewis acid sites was semi-quantified by FTIR analysis of adsorbed acetone and d<sub>3</sub>-acetonitrile molecular probes and correlated with catalytic activity and reaction selectivity in citronellal transformation in 2-propanol. We found that the ion exchange weakens the Lewis acidity of Zr “open” sites, yielding a new type of site with strength and catalytic properties similar to those of Zr “closed” sites. As a result, ion exchange shifts the reaction selectivity from carbonyl-ene cyclization to isopulegol towards MPV reduction to citronellol.

## 2. Experimental

### 2.1 Catalysts Preparation

Synthesis of Zr-beta-1: 35.17 g of tetraethyl orthosilicate (TEOS, 100%, VWR chemicals) was mixed with 35.46 g of 35 wt.% tetraethylammonium hydroxide (TEAOH, Thermo Scientific) and stirred for 2 hours at room temperature. Meanwhile, 0.729 g of anhydrous zirconium(IV) chloride (99.9%, Sigma Aldrich) was dissolved in 1.50 ml of distilled water and added dropwise to the TEOS-TEAOH mixture. Then, 1.000 g of beta seeds (zeolite beta CP811E Si/Al=150, Zeolyst Int., dealuminated according to ref.[29]) was added, followed by 3.52 g of 40 wt.% HF (VWR chemicals). The resulting gel (SiO<sub>2</sub>: TEAOH: H<sub>2</sub>O: ZrO<sub>2</sub>: HF= 100: 50: 870: 1.85: 50) was homogenized with a spatula and transferred to a Teflon-lined autoclave (90 ml) before heating at 140 °C under static conditions for 17 days. Subsequently, the solid product was recovered by centrifugation, washed with distilled water, dried at 60 °C, and calcined in air at 550 °C (2 °C/min) for 6 hours. The sample was denoted as Zr-beta-1.

Synthesis of Zr-beta-2: 28.16 g of TEOS (98%, Thermo Scientific) and 31.79 g of TEAOH (Thermo Scientific) were mixed for 15 minutes at room temperature. Then, 0.588 g zirconium(IV) isopropoxide (Zr (OiPr)<sub>4</sub>, Si/Zr=75 in the synthesis mixture) was added to the mixture and stirred overnight. Subsequently, 3.02 g 50 wt.% HF (VWR chemicals) and 0.281 g of beta seeds (zeolite beta CP811E Si/Al=150, Zeolyst Int., dealuminated according to ref.[29]), dispersed in 2.7 g of distilled water, were added to the synthesis

mixture. The resulting gel ( $\text{SiO}_2$ : TEAOH:  $\text{H}_2\text{O}$ :  $\text{ZrO}_2$ : HF= 100: 56: 842: 1.33: 54) was transferred to a Teflon-lined autoclave and heated at 140 °C for 20 days. After crystallization, the product was filtered, washed with 500 ml of distilled water, dried at 60 °C overnight, and calcined in air at 550 °C (2 °C/min) for 6 hours. This sample was denoted as Zr-beta-2.

Ion exchange: Zr-beta samples were ion-exchanged with  $\text{Li}^+$ ,  $\text{Na}^+$  or  $\text{Cs}^+$  cations, according to the method reported by Otomo et al. [39]. The activated (2 °C/min, 450 °C, static air, 6 h) zeolite powder (0.3g) was introduced into 1 mol/l alkali nitrate solution ( $\text{MNO}_3$ ,  $\text{M}=\text{Li}$ ,  $\text{Na}$ ,  $\text{V}=30\text{ml}$ ,  $\text{M}=\text{Cs}$ ,  $\text{V}=9\text{ ml}$ ), ( $\text{NaNO}_3$  (Lachner, Czech Republic, 99.5%),  $\text{LiNO}_3$  (Thermo Scientific, 99%),  $\text{CsNO}_3$  (Thermo Scientific, 99.8%)), and the mixture was stirred at 450 rpm, for 3 hours, at room temperature. Subsequently, the suspension was centrifuged and redispersed in a fresh nitrate solution. This ion exchange was repeated 3 times. Subsequently, the solid products were washed 2 times with deionized water. The washed samples were then dried at 60 °C overnight and calcined at 450 °C for 6 h using a temperature ramp of 2 °C/min to decompose leftover nitrates. The zeolite treated by  $\text{MNO}_3$  solution was denoted as Zr-beta-X- $\text{M}^+$  ( $\text{X}=1,2$ ;  $\text{M} = \text{Na}$ ,  $\text{Li}$ ,  $\text{Cs}$ ). For the Zr-beta-1  $\text{Na}^+4\text{x}$  sample, the ion exchange procedure was repeated 4 times, stirring for 24 h in each step.

## 2.2. Catalyst characterization

Powder X-ray diffraction (XRD) analysis was performed on a Bruker D8 Advance diffractometer, equipped with a LYNXEYE XE-T detector, and with  $\text{Cu K}\alpha$  radiation ( $\lambda = 1.5406\text{ \AA}$ ). Powdered samples were scanned over a  $2\theta$  range of 3–40° with a step size of 0.021° and 0.05 s per step.

For all samples, surface area and pore volume values were measured by  $\text{N}_2$  physisorption analysis at –196 °C on a Micromeritics 3Flex Surface Analyzer. Before each measurement, the samples were outgassed on a Micromeritics Smart Vac Prep instrument under vacuum, heating from room temperature to 110 °C at 1 °C/min until the residual pressure reached 13.3 Pa and maintaining these conditions for 1 h. Then, the temperature was increased to 250 °C at 1 °C/min and held for 8 h. BET surface area ( $S_{\text{BET}}$ ) was calculated using the Brunauer-Emmett-Teller (BET) method based on adsorption data in the relative pressure range  $p/p_0 = 0.05\text{--}0.20$ . Micropore volume ( $V_{\text{mic}}$ ) and external surface area ( $S_{\text{ext}}$ ) were calculated using the t-plot method with Harkins-Jura reference isotherm. Total adsorption capacity ( $V_{\text{tot}}$ ) was estimated from the amount of  $\text{N}_2$  adsorbed at a relative pressure of  $p/p_0 = 0.95$ .

Elemental composition was determined by inductively coupled plasma mass spectrometry (ICP-MS) on an Agilent 7900 ICP-MS spectrometer (Agilent Technologies, Inc., USA.). For ICP-MS, 50 mg of each sample was acid-digested by a mixture of 1.8 ml of  $\text{HNO}_3$  (67–69%, ANALPURE), 5.4 ml of  $\text{HCl}$  (34–37%, ANALPURE) and 1.8 ml of  $\text{HF}$  (47–51%, ANALPURE), transferred into a closed Teflon vessel (60 ml, type DAP60), and heated at 210 °C (5 °C/min) for 25 min in a microwave oven (Speedwave XPERT, Berghof). Once the sample cooled down, excess  $\text{HF}$  was treated with  $\text{H}_3\text{BO}_3$  before heating again at 190 °C (5 °C/min) for 10 min in a microwave. Then, the final solution was diluted with distilled water for analysis.

Lewis acid sites in zeolite samples were characterized by FTIR spectroscopy using adsorbed probe molecules, either acetone (AC, 100%, VWR Chemicals) or  $\text{d}_3$ -acetonitrile ( $\text{CD}_3\text{CN}$ ,  $\geq 99.9\%$ , Sigma Aldrich). The samples were pressed into self-supporting wafers with 8–12  $\text{mg}\cdot\text{cm}^{-2}$  density and activated *in situ* for 5 h at 450 °C under  $10^{-3}$  Pa vacuum.  $\text{CD}_3\text{CN}$  adsorption was performed at room temperature for 20 min at 500 Pa partial pressure, followed by desorption for 20 min at the same temperature. AC adsorption was performed stepwise (dose-by-dose) at room temperature. AC adsorption at 500 Pa partial pressure and

room temperature for 20 min was followed by desorption for 20 min at 50 °C. FTIR spectra were recorded on a Nicolet iS50 spectrometer equipped with a DTGS detector, at 4 cm<sup>-1</sup> resolution, accumulating 64 scans per spectrum. Spectral processing was performed using Thermo Scientific OMNIC 9.0 software. To quantify the fraction of Zr Lewis acid sites in different configurations, all spectra were normalized to 10 mg·cm<sup>-2</sup> sample density, baseline-corrected, and deconvoluted using a Gaussian line shape according to ref.[30] for CD<sub>3</sub>CN and ref.[29] for AC. The centers of the bands were fixed within 5 cm<sup>-1</sup>, and the total widths at half maximum ranged from 5 to 20 cm<sup>-1</sup>. The relative fractions of Zr Lewis acid sites or different strengths of interaction with acetone were then estimated from the ratios of the peak areas of the characteristic bands at 1710 and 1698 cm<sup>-1</sup> in the FTIR spectra of adsorbed AC.

Scanning electron microscopy (SEM) images were acquired under a Thermo Fisher Scientific Scios 2 DualBeam FIB-SEM equipped with a Schottky-type field emission gun at 12 kV accelerating voltage, 1.6 nA beam current, and 6 mm working distance. For some samples, elemental composition was semi-quantitatively analyzed by energy-dispersive X-ray spectroscopy (EDX) using a Thermo Fisher Scientific UltraDry X-ray detector integrated into the SEM system. Data were collected at 12 kV accelerating voltage, 1.6 nA beam current and 6 mm working distance. All samples were mounted on conductive carbon tape attached to the SEM aluminum stub holder.

### 2.3. Catalytic tests

Catalytic MPV reduction of citronellal was used as a model reaction to monitor the effect of ion exchange with an alkali cation. Before each test, the catalyst was activated at 450 °C (2 °C/min) for 6 h in a muffle furnace under static air. For each experiment, 20 mg of activated catalyst was added to 6 ml (78 mmol) of 2-propanol (≥98%, VWR Chemicals) in a 25-ml three-neck round-bottom flask. The flask fitted with a reflux condenser, a magnetic stirrer and a septum was placed in a Starfish™ workstation. Then, the reaction mixture was heated to 70 °C under magnetic stirring (450 rpm). Once the temperature reached and stabilized at 70 °C, a mixture of 2.22 mmol citronellal (96%, Thermo Scientific) and 1.29 mmol mesitylene (98%, Sigma Aldrich, internal standard) was added to the flask to initiate the reaction. The reaction mixture was sampled every hour for 6 h. Once the samples were taken, they were immediately cooled and centrifuged (5000 rpm, 3 min) to separate the catalyst. Subsequently, the samples were analyzed on an Agilent GC-7890 system equipped with a VF-WAXms column (30m × 0.25mm × 1.0 μm) and a flame ionization detector, using N<sub>2</sub> as carrier gas.

Citronellal conversion (X), product yield (Y<sub>p</sub>, P=citronellol, isopulegols, citronellal diisopropyl acetal), the corresponding selectivity (S<sub>p</sub>) and turn-over-frequency (TOF) per 1 Zr atom were calculated using the following formulas:

$$(1) \text{ Citronellal conversion: } X (\%) = \frac{n_0 - n_a}{n_0}.$$

$$(2) \text{ Product yield: } Y_p (\%) = \frac{n_p}{n_0},$$

$$(3) S_p (\%) = \frac{Y_p}{X}, \text{ Selectivity: product yield as a function of citronellal conversion; the slope is the average selectivity.}$$

$$(4) \text{ TOF (h}^{-1}\text{)} = \frac{n_p}{n_{Zr} \times t}$$

where  $n_0$  stands for the initial molar amount of citronellal;  $n_p$ , for the molar amount of the product in the sample;  $n_{Zr}$ , for the molar amount of Zr atoms in the reaction mixture; and  $t$ , for the time when the sample was taken from the reaction mixture.

In the catalyst recycling test, the catalyst was isolated after 6 h of the catalytic run. In an open vial, the catalyst was dried at 25°C overnight in a hood prior to activation at 450 °C (2 °C/min), for 6 h, in a muffle furnace, and reused in the next run. The amounts of the reagents were adjusted to the exact amount of the recycled catalyst after activation. In the hot filtration test, the reaction mixture was filtered, after 1 h, using a 45 µm Teflon membrane syringe filter, into a clean preheated flask to remove the catalyst, and the filtrate was stirred at 70 °C and sampled.

### 3. Results and discussion

#### 3.1. Catalyst characterization

This study aims to elucidate how ion exchange with alkali metal cations influence catalytic properties of Al-free Zr-beta zeolites in the MPV reduction of citronellal to citronellol. For this purpose, we hydrothermally synthesized two Al-free Zr-beta zeolites with different Si/Zr ratios (Table 1) and ion-exchanged with Li<sup>+</sup>, Na<sup>+</sup> or Cs<sup>+</sup> cations using the corresponding nitrate solutions. Acid site strength of the resulting catalysts was thoroughly characterized by FT-IR spectroscopy of adsorbed acetone (AC) and d<sub>3</sub>-acetonitrile (CD<sub>3</sub>CN) molecular probes, while the catalytic performance of Zr-beta-X-M<sup>+</sup> (X=1,2; M = Na, Li, Cs) series was tested in the citronellal reaction with 2-propanol in which MPV reduction competes with citronellal carbonyl-ene cyclization and acetalization (Figure 1).

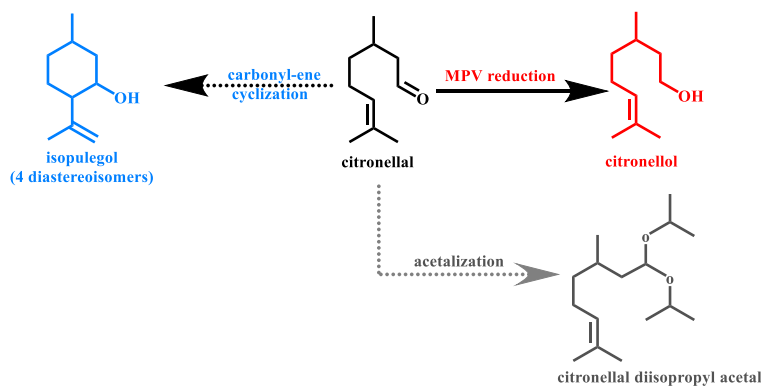


**Figure 1. Reaction pathways of citronellal transformation in 2-propanol over Zr-beta zeolites**

The X-ray diffraction (XRD) patterns of both Zr-beta-1 and Zr-beta-2 catalysts, shown in Figure S1, supporting information (SI), correspond to the beta topology, with no additional crystalline phases. The shape of the broad peak around 7.7° 2-theta indicates that Zr-beta-1 contains beta polymorphs A and B in an approximately 40/60 ratio. For Zr-beta-2, the polymorph A/B ratio is estimated at 50/50 [41]. After ion exchange, all catalysts displayed unaltered XRD patterns. These results suggest that the crystalline structures of Zr-beta zeolites remained unaffected and that no additional phases were formed upon ion exchange.

**Table 1: ionic radii in pm of elements, ion-exchanged amounts, textural properties and chemical composition of the samples**

Sample	M <sup>+</sup> effective ionic radius <sup>a</sup>	M <sup>+</sup> /Zr	Si/Zr <sup>b</sup>	S <sub>BET</sub>	S <sub>ext</sub>	V <sub>micro</sub>	V <sub>total</sub>
	pm						
Zr-beta-1	--	0	58	650	78	0.23	0.29
Zr-beta-1-Li <sup>+</sup>	68	0.20	58	669	87	0.23	0.30



<b>Zr-beta-1-Na<sup>+</sup></b>	95	0.15 <sup>c</sup>	58	614	79	0.21	0.27
<b>Zr-beta-1-Na<sup>+</sup>4x</b>	95	0.31 <sup>c</sup>	58	n.a. <sup>d</sup>	n.a.	n.a.	n.a.
<b>Zr-beta-1-Cs<sup>+</sup></b>	169	0.34	58	628	83	0.22	0.28
<b>Zr-beta-2</b>	--	0	127	523	51	0.18	0.25
<b>Zr-beta-2-Li<sup>+</sup></b>	68	0.25	127	528	50	0.19	0.25
<b>Zr-beta-2-Na<sup>+</sup></b>	95	0.47 <sup>c</sup>	127	533	52	0.19	0.25
<b>Zr-beta-2-Cs<sup>+</sup></b>	169	0.55	127	524	44	0.19	0.23

<sup>a</sup> M<sup>+</sup> = Li<sup>+</sup>, Na<sup>+</sup>, Cs<sup>+</sup>; data taken from reference[42].

<sup>b</sup> average value from 4 ICP-MS analyses

<sup>c</sup> determined by SEM-EDX analysis, averaging analyses of 2 spots approximately 20 x 20 μm

<sup>d</sup> not analyzed because the other analyses showed no effect on textural properties

Textural properties and elemental compositions of the catalysts are outlined in Table 1. As in the XRD analysis, the BET areas and micropore volumes of the Zr-beta samples remained mostly unchanged after ion exchange, and the values are consistent with data reported in the literature [15, 29, 30]. N<sub>2</sub> adsorption-desorption isotherms of the Zr-beta catalysts (Figure S2, SI) are all type I, which is typical of microporous materials. Zr-beta-2 shows a more pronounced hysteresis loop than Zr-beta-1, highlighting that Zr-beta-2 has a slightly higher interparticle volume than Zr-beta-1, most likely resulting from differences in morphology. SEM images (Figure S3, SI) show olive-shaped aggregates in Zr-beta-1, in contrast to octahedron-like aggregates in Zr-beta-2. The aggregates averaged approximately 1 μm in size, regardless of type.

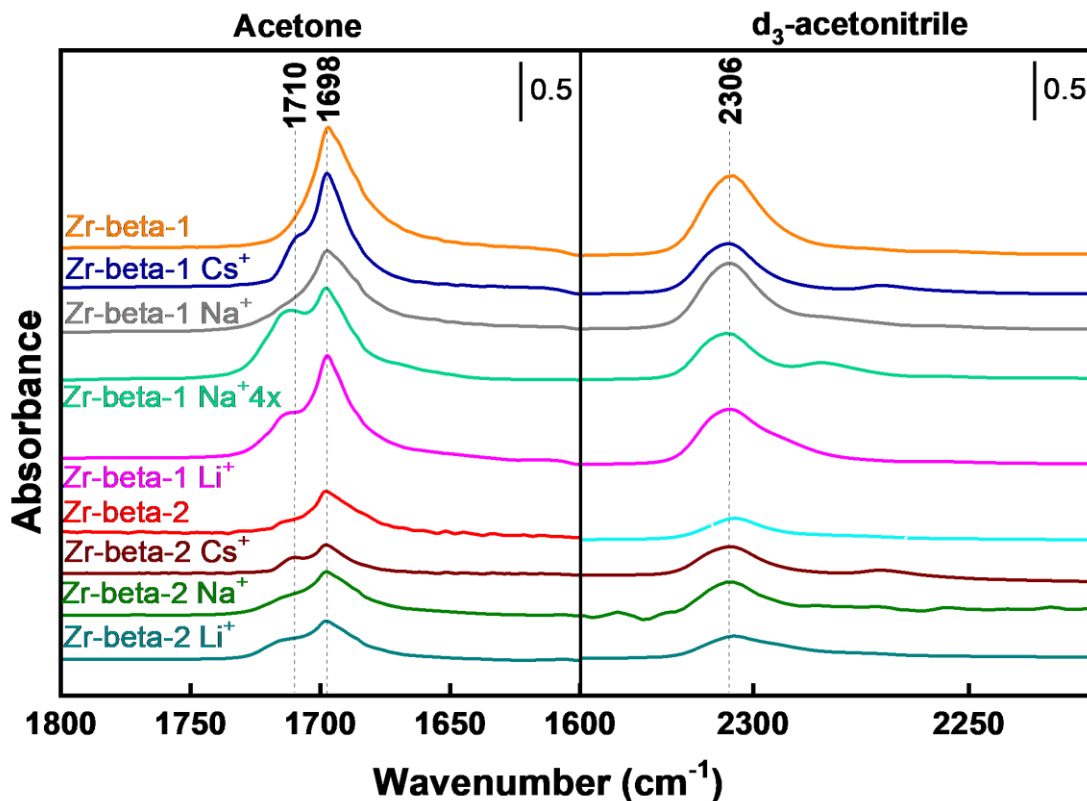


**Figure 2. FTIR spectra of the catalysts after adsorption of an excess of AC and CD<sub>3</sub>CN and subsequent desorption at room temperature**

By FT-IR spectroscopy of adsorbed AC and CD<sub>3</sub>CN, we analyzed the type, strength and amount of Lewis acid sites in Zr-beta catalysts before and after ion exchange. FT-IR spectra were collected after evacuation and activation at 450 °C, so the samples were completely dehydrated prior to probe adsorption, and the Zr coordination number should be 4 for both “closed” and “open” sites [30]. In M<sup>+</sup>-free Zr-beta catalysts, the AC probe distinguished weaker “closed” from stronger “open” Zr sites by showing characteristic  $\nu(\text{C}=\text{O})$  bands of the acetone coordinated to the Zr atom at 1712 cm<sup>-1</sup> and 1698 cm<sup>-1</sup>, respectively [29]. The band of physisorbed or H-bonded acetone  $\nu(\text{C}=\text{O})$  can be observed at 1719 cm<sup>-1</sup> (matching the position of the band of liquid acetone  $\nu(\text{C}=\text{O})$ [43]; the position of the AC gas-phase  $\nu(\text{C}=\text{O})$  band is 1731 cm<sup>-1</sup>) but vanishes upon evacuation of the sample as these acetone molecules desorb [29]. In contrast, CD<sub>3</sub>CN interacts exclusively with Zr “open” sites [30], so it is used as a complementary probe to AC. The position of the CD<sub>3</sub>CN  $\nu(\text{C}\equiv\text{N})$  vibration band in gas phase is 2265 cm<sup>-1</sup>. When CD<sub>3</sub>CN binds to a Lewis acid site, its stretching frequency  $\nu(\text{C}\equiv\text{N})$  blue-shifts, unlike AC and other carbonyl probes, where the position of the  $\nu(\text{C}=\text{O})$  band red-shifts upon interaction with the Lewis acid sites. Moreover, the blue-shift is larger than the red-shift, indicating a stronger interaction with the acid site [44, 45].

Figure 2 shows the  $\nu(\text{C}=\text{O})$  region of AC and the  $\nu(\text{C}\equiv\text{N})$  region of CD<sub>3</sub>CN adsorbed on Zr-beta-1 and Zr-beta-2 before and after ion exchange with Li<sup>+</sup>, Na<sup>+</sup> or Cs<sup>+</sup>. In both Zr-beta-1 and Zr-beta-2, intensity is redistributed between the two AC bands upon ion exchange; the band at 1698 cm<sup>-1</sup>, assigned to acetone coordinated to stronger “open” Lewis acid sites, becomes weaker, whereas the higher-frequency band at 1710 cm<sup>-1</sup>, initially assigned to acetone coordinated to weaker “closed” Lewis acid sites, gains intensity. This effect is particularly evident in Cs<sup>+</sup>-exchanged samples (e.g., Zr-beta-2 area 1.3 vs. Zr-beta-2-Cs<sup>+</sup> 1.6, Table S1, SI, Figure 3) and Zr-beta-1-Na<sup>+</sup>4x. In these materials, the 1710 cm<sup>-1</sup> band gains intensity, whereas the 1698 cm<sup>-1</sup> band becomes weaker. These changes in band intensity are not directly proportional because the two bands likely have different molar absorption coefficients, similarly as it was reported for the “open” and “closed” Sn sites [32] and Hf sites [46], probed by CD<sub>3</sub>CN. In contrast, the CD<sub>3</sub>CN spectra show only moderate variations in intensity of the band at 2306 cm<sup>-1</sup> upon ion exchange. Band intensity does not decrease in parallel with the strong changes observed in the AC 1698 cm<sup>-1</sup> band. In some samples, such as Zr-beta-2-Na<sup>+</sup> and Zr-beta-2-Cs<sup>+</sup>, the CD<sub>3</sub>CN band intensity even increases slightly. Combined, our AC and CD<sub>3</sub>CN IR data indicate that ion exchange does not convert “open” Zr sites into structurally different sites but alters the strength of the interaction between probe molecules and existing Zr Lewis acid sites.

The differences in AC and CD<sub>3</sub>CN responses to these perturbations may be explained by the type of their electron-donor orbitals and the resulting interaction with the Zr centers [47]. AC coordinates to Zr Lewis acid sites via donation from an oxygen lone pair predominantly associated with an sp<sup>2</sup>-hybridized orbital, whereas CD<sub>3</sub>CN binds through donation from a nitrogen lone pair located in an sp-hybridized orbital [48]. While a rigorous comparison of absolute lone-pair energies of the probe molecules is complicated by differences between the atoms, lone pairs with lower s-character tend to have higher energy and basicity (sp<sup>3</sup> > sp<sup>2</sup> > sp) [48, 49]. In line with this notion, AC has a higher proton affinity (812 kJ/mol [50, 51]) than CD<sub>3</sub>CN (779 kJ/mol [50]), qualitatively reflecting the stronger electron-donor character of acetone. In this context, the oxygen lone pair in AC may be more effective in interacting with vacant orbitals of Zr centers and more sensitive to subtle changes in the local electrostatic environment.

Upon ion exchange, partial electrostatic shielding of Zr sites by nearby alkali cations is directly reflected in the  $\nu(\text{C}=\text{O})$  vibration region of the IR spectra (Figure 2), suggesting a noticeable weakening of the acid site-acetone interaction. In contrast, CD<sub>3</sub>CN binds to Zr sites through donation of the lone pair located in an sp-hybridized orbital. This interaction is less sensitive to moderate perturbations of Zr Lewis acidity induced by ion exchange. As a result, CD<sub>3</sub>CN is less effective in discriminating between Lewis acid sites of similar



strength and, instead, primarily reports on the presence of accessible Lewis acid sites, a population that is largely preserved upon ion exchange.

The increased intensity of the AC band at  $1710\text{ cm}^{-1}$  reflects the presence of a new type of Lewis acid sites. These Lewis acid sites show weaker interactions with AC because this band is closer to that of non-interacting acetone and evolves only after saturation of the  $1698\text{ cm}^{-1}$  band when acetone is introduced in small doses to the cell (Figure 3). In our previous study [29] on  $M^+$ -free Zr-beta catalysts, we ascribed this band to Zr “closed” sites; most likely, this band probes “closed” sites in alkali ion-free Zr-beta-1 and Zr-beta-2. Upon ion exchange, a fraction of “open” sites may be converted into “closed” sites. However, this scenario is unlikely for two main reasons. First, ion exchange is performed in aqueous medium, so the opposite transformation should occur under these conditions [52]. Second, conversion into “closed” sites should induce the loss of Brønsted character, occluding the alkali cation, which would reverse the process again [33]. Conversely, we postulate that ion exchange decreases the acidity strength of the “open” Zr sites to that of the “closed” Zr sites, thus changing their spectroscopic features and catalytic properties (*vide infra*). This interpretation is supported by the findings of Gao et al. [40] on Zr-Al-beta catalysts.

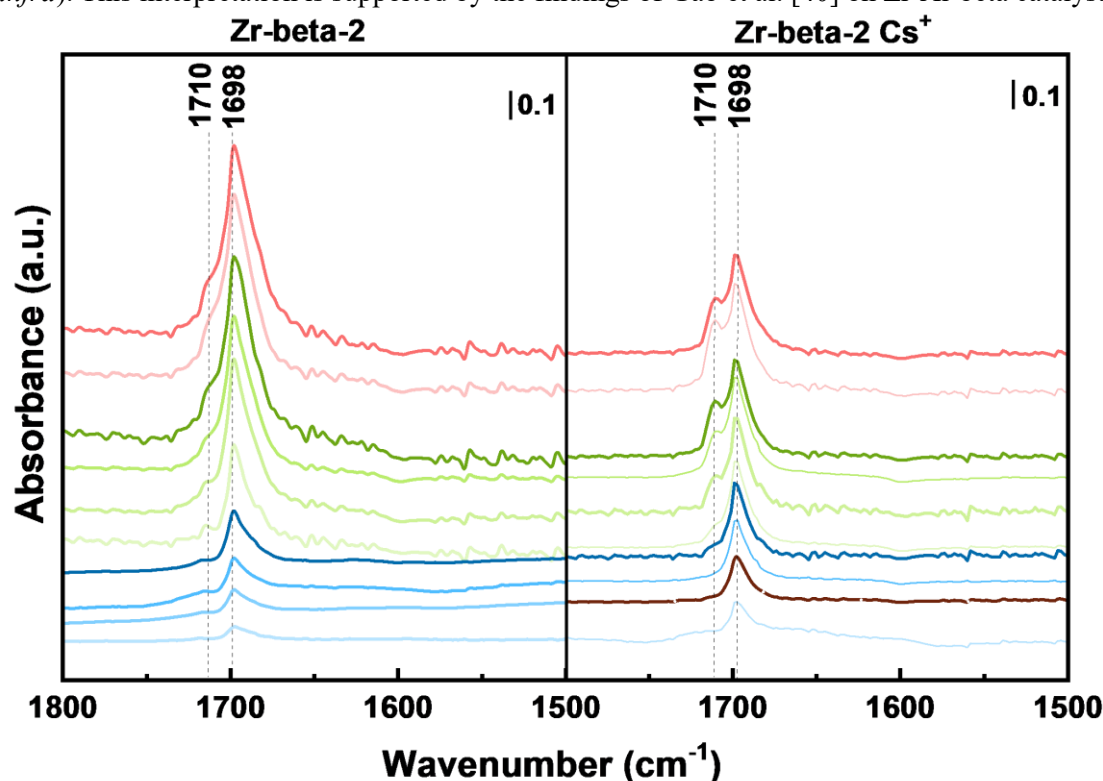


Figure 3. Dose-by-dose adsorption of acetone on Zr-beta-2 (left) and Zr-beta-2- $\text{Cs}^+$  (right) at room temperature

### 3.2. Catalytic performance

The effect of ion exchange with an alkali cation on the catalytic performance of Zr-beta was assessed in a Lewis acid-catalyzed reaction of citronellal with/in 2-propanol over two sets of ion-exchanged Zr-beta catalysts in liquid phase at  $70\text{ }^{\circ}\text{C}$ . In addition, we performed a blank experiment with no catalyst and a set of reference experiments over Zr-beta-2 with nitrate salts added directly to the reaction mixture. Under these conditions, citronellal undergoes three main reaction pathways, namely (i) MPV reduction, yielding citronellol and acetone, (ii) intramolecular carbonyl-ene cyclization, yielding a pool of isopulegol isomers,

and (iii) acetalization, yielding citronellal diisopropyl acetal (hereafter denoted as *acetal*). Furthermore, we observed small amounts of citronellal isopropyl hemiacetal and several minor products (<1 % yield each), which were identified as citronellal isomerization products, in some samples. In a reference experiment without catalyst, no conversion was observed after 6 h.

Figure 4 shows the citronellol selectivity of parent and ion-exchanged Zr-beta-1 and Zr-beta-2 catalysts. The corresponding citronellal conversion and isopulegol selectivity curves are provided in Figure S4 and Figure S5, SI, respectively. The results demonstrate that selectivity is independent of conversion, confirming that ion exchange does not alter the reaction scheme and that MPV reduction and carbonyl-ene cyclization remain parallel reactions [29].

For both Zr-beta-1 and Zr-beta 2, citronellol selectivity follows a clear trend: parent Zr-beta-1 (26%) < Zr-beta-1- $\text{Na}^+$  (40%) < Zr-beta-1- $\text{Li}^+$  (50%) < Zr-beta-1- $\text{Cs}^+$  (69%). This trend results from the increase in MPV reduction TOF upon ion exchange (e.g., Zr-beta-1 citronellol formation TOF  $60 \text{ h}^{-1}$  vs. Zr-beta-1- $\text{M}^+$  TOF 76-113; Table 2) and cannot be explained by the cation size. Nevertheless, the TOF of citronellol formation over Zr-beta-1, in particular, increases linearly with the  $\text{Na}^+/\text{Zr}$  ratio, that is, the degree of ion exchange (Figure S6 top, SI). Simultaneously, the TOF of isopulegol formation strongly decreases, thus accounting for the higher citronellol selectivity (77 %) of Zr-beta-1- $\text{Na}^+4x$ . Moreover, Zr-beta-1- $\text{Li}^+$  and Zr-beta-1- $\text{Cs}^+$  also follow this trend (Figure S6, bottom), suggesting that the degree of ion-exchange drives the reaction, regardless of the cation. For Zr-beta-2 catalysts, this trend is not so straightforward but likely derives from the lower Zr content and, thus, lower activity. The increase in the MPV reduction selectivity aligns with the spectroscopic observation that the stronger Zr “open” sites become weaker upon ion exchange. These weaker Zr “open” sites catalyze MPV reduction.

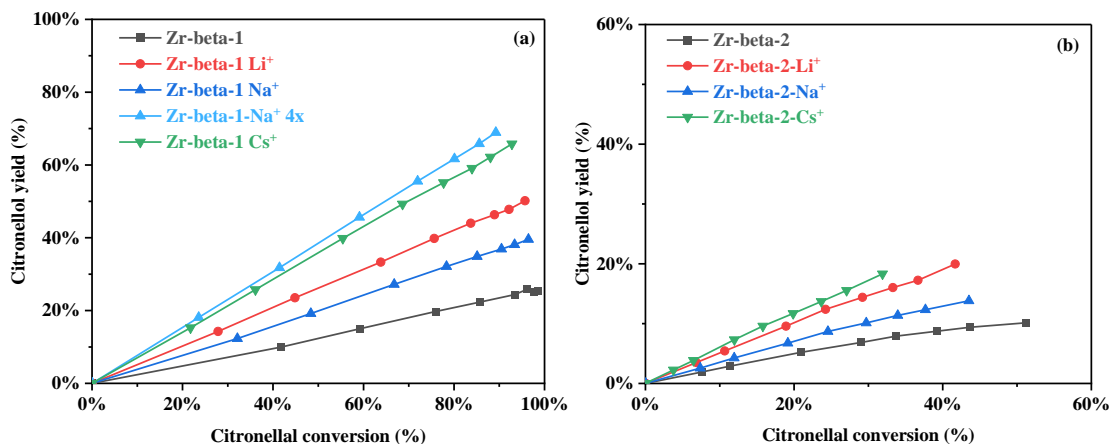


**Figure 4. Citronellol yield as a function of citronellal conversion over (a) Zr-beta-1 and (b) Zr-beta-2 catalysts**

To confirm this interpretation, we plotted the MPV reduction and carbonyl-ene TOF calculated from 1h datapoints against integrated areas of the AC band at  $1710 \text{ cm}^{-1}$ , which probes the weaker Zr “closed” sites and the ion-exchanged Zr sites that catalyze the MPV reaction (Figure 5 (a)), and of the  $\text{CD}_3\text{CN}$  band at  $2306 \text{ cm}^{-1}$ , which probes the non-exchanged Zr “open” sites (Figure 5 (b)). MPV reduction TOF is proportional to intensity of the band of the weaker sites and, accordingly, to site concentration. The correlation between the intensity of the band of the stronger Zr “open” sites and the carbonyl-ene cyclization TOF is significant only in Zr-beta-1 catalysts. A possible explanation is the slow diffusion of the product isopulegol out of these sites due to its substituted cyclohexane structure, in contrast to citronellal and

citronellol, which are linear molecules. This slow diffusion manifests more strongly in catalysts with a low Zr content (Zr-beta-2 set) and may also account for slight differences in the correlation between the TOF of MPV reduction and the intensity of the band characteristic of “closed” sites of individual sets of Zr-beta-1 and Zr-beta-2 catalysts (Figure 5 (a)).

**Table 2. Selectivity and TOF of the citronellal (2.2 mmol) reaction with/in 2-propanol (78 mmol) over 20 mg of catalyst at 70 °C**

Catalyst	TOF <sup>a</sup>		Selectivity <sup>b</sup>		
	Isopulegol	Citronellol	Isopulegol	Citronellol	Acetal
	h <sup>-1</sup>	h <sup>-1</sup>	(%)	(%)	(%)
<b>Zr-beta-1</b>	<b>179</b>	<b>60</b>	<b>73</b>	<b>26</b>	<b>2</b>
<b>Zr-beta-1-Li<sup>+</sup></b>	<b>94</b>	<b>95</b>	<b>51</b>	<b>52</b>	<b>1</b>
<b>Zr-beta-1-Na<sup>+</sup></b>	<b>121</b>	<b>76</b>	<b>59</b>	<b>41</b>	<b>1</b>
<b>Zr-beta-1-Na<sup>+</sup>4x</b>	<b>33</b>	<b>113</b>	<b>23</b>	<b>77</b>	<b>0</b>
<b>Zr-beta-1-Cs<sup>+</sup></b>	<b>50</b>	<b>104</b>	<b>32</b>	<b>71</b>	<b>1</b>
<b>Zr-beta-2</b>	<b>77</b>	<b>25</b>	<b>71</b>	<b>21</b>	<b>2</b>
<b>Zr-beta-2-Li<sup>+</sup></b>	<b>52</b>	<b>47</b>	<b>51</b>	<b>48</b>	<b>0</b>
<b>Zr-beta-2-Na<sup>+</sup></b>	<b>67</b>	<b>37</b>	<b>61</b>	<b>33</b>	<b>4</b>
<b>Zr-beta-2-Cs<sup>+</sup></b>	<b>28</b>	<b>33</b>	<b>41</b>	<b>58</b>	<b>0</b>
<b>No catalyst</b>	<b>0</b>	<b>0</b>	<b>--</b>	<b>--</b>	<b>--</b>
<b>Zr-beta-2 + LiNO<sub>3</sub></b>	<b>25</b>	<b>30</b>	<b>20</b>	<b>25</b>	<b>36</b>
<b>Zr-beta-2 + NaNO<sub>3</sub></b>	<b>24</b>	<b>35</b>	<b>25</b>	<b>42</b>	<b>22</b>
<b>Zr-beta-2 + CsNO<sub>3</sub></b>	<b>28</b>	<b>33</b>	<b>29</b>	<b>31</b>	<b>18</b>
<b>No catalyst + LiNO<sub>3</sub></b>	<b>&lt;1</b>	<b>0</b>	<b>3</b>	<b>0</b>	<b>61</b>

<sup>a</sup> TOF evaluated from 1 h datapoints

<sup>b</sup> Selectivity is calculated as the slope of yield vs. conversion curves in Figure 4, Figure 6. Balance to 100% represents a cumulative selectivity to citronellal isopropyl hemiacetal and citronellal isomerization side products.

The stability of ion-exchanged Zr-beta was assessed in a 3-run recycling test with the most citronellol-selective catalyst, Zr-beta-1-Na<sup>+</sup>4x (Figure S7, SI), and in a hot filtration test. The conversion curves remained unchanged throughout the 3 consecutive runs. Citronellol selectivity (assessed as in Table 2) dropped from 77% in the 1<sup>st</sup> run to 70% in the 2<sup>nd</sup> run, without changing in the 3<sup>rd</sup> run. So, after the initial equilibration, the catalyst was stable under the reaction conditions, without significant Na<sup>+</sup> leaching; otherwise, the selectivity of MPV reduction would have continued to decrease. Based on the results from the hot filtration test, the composition of the reaction mixture does not change after removing the catalyst, thus confirming the purely heterogeneous character of the catalytic reaction.

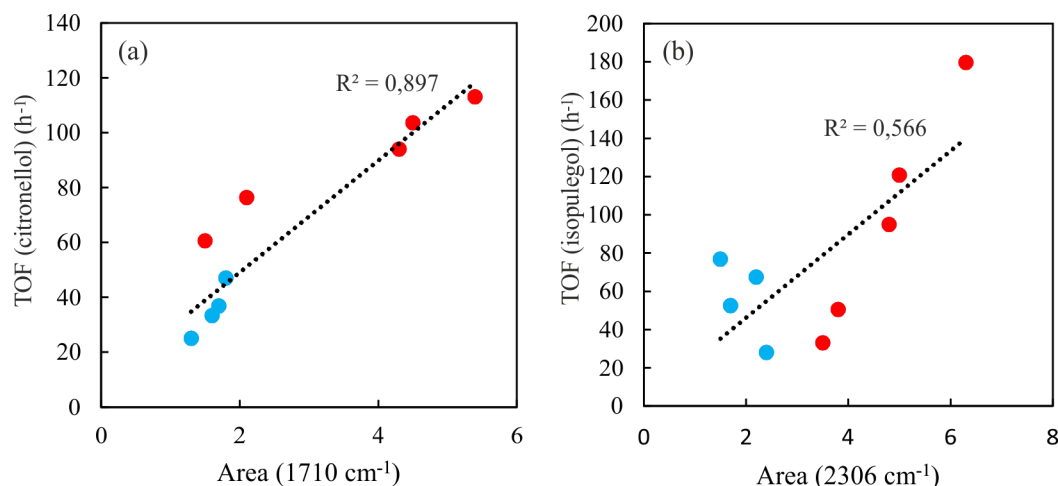


**Figure 5: Variation of TOF of (a) citronellol formation as a function of AC 1710 cm<sup>-1</sup> band area representing weaker Zr sites and (b) isopulegol formation as a function of CD<sub>3</sub>CN 2306 cm<sup>-1</sup> band area representing stronger Zr “open” sites in Zr-beta-1 (red) and Zr-beta-2 (blue).**

We also assessed the effect of adding the alkali metal salt directly to the reaction mixture. For this purpose, we mixed parent Zr-beta-2 catalyst with 0.1 citronellal-based molar equivalent of LiNO<sub>3</sub>, NaNO<sub>3</sub> and CsNO<sub>3</sub>, that is, 0.22 mmol of each salt, in the catalytic experiment. MPV reduction TOF slightly increased (e.g., Zr-beta-2 with added NaNO<sub>3</sub> 35 h<sup>-1</sup> vs. no salt 25 h<sup>-1</sup>) while the carbonyl-ene TOF decreased strongly (e.g., Zr-beta-2 with added NaNO<sub>3</sub> 24 h<sup>-1</sup> vs. no salt 77 h<sup>-1</sup>), with negligible differences between the 3 nitrate salts (Table 2). These results confirm that the size of the cation does not affect selectivity under these conditions.

Suppression of carbonyl-ene cyclization indicates that Zr “open” sites were ion exchanged also *in situ*; nevertheless, citronellol selectivity increased only slightly (Table 2, Figure 6, Figure S8, SI) because the presence of excess nitrate salt strongly promoted acetalization (e.g., 22% acetal selectivity over Zr-beta-2 with added NaNO<sub>3</sub> vs. 2% without salt) and side citronellal isomerization. The control experiment with only LiNO<sub>3</sub> (without zeolite catalyst) yielded mostly citronellal diisopropyl acetal (6.6% yield after 6 h), with traces of isopulegol and no citronellol.

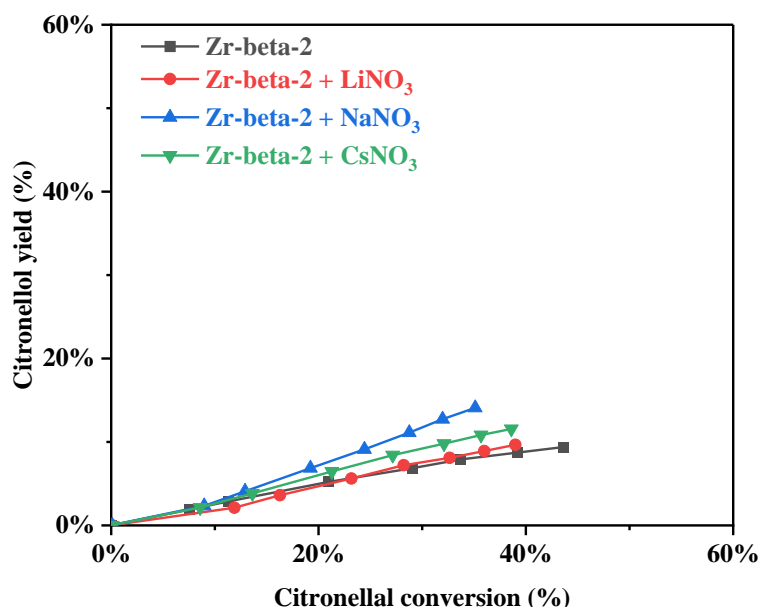


Figure 6. Variation of citronellol yield as a function of citronellal conversion over Zr-beta-2

#### 4. Conclusion

Ion exchange of Zr-beta zeolite “open” sites with  $\text{Li}^+$ ,  $\text{Na}^+$  or  $\text{Cs}^+$  ions, increases the concentration of Lewis acid sites, which exhibit weaker interactions with carbonyl compounds. Whether they correspond to  $\text{M}^+$  cations, perturbed “open” Zr sites or Zr sites influenced by nearby alkali cations cannot be resolved unambiguously from the available data, but these weaker sites share both spectroscopic characteristics, that is, an adsorbed acetone band at  $1710\text{ cm}^{-1}$ , and catalytic properties with Zr “closed” sites. Similarly to the Zr “closed” sites, ion-exchanged Zr “open” sites catalyze MPV reduction of citronellal, while non-ion-exchanged “open” sites catalyze the competing reaction, carbonyl-ene cyclization. As a result, ion exchange significantly increases MPV reduction selectivity (e.g., Zr-beta-1 26% vs. Zr-beta-1- $\text{Cs}^+$  71%), but not the overall rate of citronellal conversion (e.g., 97.5% conversion over Zr-beta-1 after 6 h vs. 88% conversion over Zr-beta-1- $\text{Cs}^+$  after 6 h). MPV reduction TOF is proportional to the intensity of the acetone band characteristic of weaker Zr sites and, as such, to the concentration of the sites. The size of the cation does not affect the catalytic properties.

#### Declaration of Competing Interest

Co-authors have no conflicts of interest to disclose.

#### Acknowledgements

J.P. and M.S. acknowledge the Ministry of Education, Youth and Sport of the Czech Republic for the ERC CZ grant LL2104, and J.X. and J.C. acknowledge the Ministry of Education, Youth and Sports of the Czech Republic for the ERDF/ESF grant TECHSCALE No. CZ.02.01.01/00/22\_008/0004587 for funding this research. The authors also acknowledge the Charles University Centre of Advanced Materials (CUCAM—OP VVV Excellent Research Teams, no. CZ.02.1.01/0.0/0.0/15\_003/0000417) for providing instrumental facilities enabling this research. The authors thank Dr. Martin Kubů for performing the  $\text{N}_2$  physisorption and ICP-MS analyses and Dr. Monika Remzová for the SEM-EDX analyses. The authors also express their gratitude to Dr. Carlos V. Melo for editing the manuscript.

## Appendix A. Supplementary material

Supporting information: additional characterization and catalytic data.

### Data Availability

Presented data can be found in the ZENODO repository.

### References

- [1] J. Přech, P. Pizarro, D.P. Serrano, J. Čejka, From 3D to 2D zeolite catalytic materials, *Chem. Soc. Rev.*, 47 (2018) 8263-8306, <https://doi.org/10.1039/C8CS00370J>
- [2] Y. Li, J. Yu, New stories of zeolite structures: Their descriptions, determinations, predictions, and evaluations, *Chem. Rev.*, 114 (2014) 7268-7316, <https://doi.org/10.1021/cr500010r>
- [3] V.L. Sushkevich, D. Palagin, I.I. Ivanova, With Open Arms: Open Sites of ZrBEA Zeolite Facilitate Selective Synthesis of Butadiene from Ethanol, *ACS Catal.*, 5 (2015) 4833-4836, <https://doi.org/10.1021/acscatal.5b01024>
- [4] O. Singh, C. Samanta, L. Kustov, L. Pinard, Zeolite catalysts for biomass valorization: Tuning of active sites for promoting reactivity, *Catal. Rev.*, (2024) 1-103, <https://doi.org/10.1080/01614940.2024.2387535>
- [5] A. Corma, L.T. Nemeth, M. Renz, S. Valencia, Sn-zeolite beta as a heterogeneous chemoselective catalyst for Baeyer–Villiger oxidations, *Nature*, 412 (2001) 423-425, <https://doi.org/10.1038/35086546>
- [6] Y. Zhu, G. Chuah, S. Jaenicke, Al-free Zr-zeolite beta as a regioselective catalyst in the Meerwein–Ponndorf–Verley reaction, *Chem. Commun.*, (2003) 2734-2735, <https://doi.org/10.1039/B309191K>
- [7] M. Taramasso, G. Perego, B. Notari, Preparation of porous crystalline synthetic material comprised of silicon and titanium oxides, *US Pat.* 4410501, 1983.
- [8] X. Liu, Z. Zhu, Synthesis and catalytic applications of advanced Sn- and Zr-zeolites materials, *Adv. Sci.*, 11 (2024) 2306533, <https://doi.org/10.1002/advs.202306533>
- [9] M. Koehle, R.F. Lobo, Lewis acidic zeolite Beta catalyst for the Meerwein–Ponndorf–Verley reduction of furfural, *Catal. Sci. Technol.*, 6 (2016) 3018-3026, <https://doi.org/10.1039/C5CY01501D>
- [10] S.L. Suib, J. Přech, E. Szaniawska, J. Čejka, Recent Advances in Tetra- (Ti, Sn, Zr, Hf) and Pentavalent (Nb, V, Ta) Metal-Substituted Molecular Sieve Catalysis, *Chem. Rev.*, 123 (2023) 877-917, <https://doi.org/10.1021/acs.chemrev.2c00509>
- [11] J. Přech, Catalytic performance of advanced titanasilicate selective oxidation catalysts - a review, *Catal. Rev.*, 60 (2018) 71-131, <https://doi.org/10.1080/01614940.2017.1389111>
- [12] J. Přech, M.A. Carretero, J. Čejka, Baeyer–Villiger Oxidation of Cyclic Ketones by Using Tin–Silica Pillared Catalysts, *ChemCatChem*, 9 (2017) 3063-3072, <https://doi.org/10.1002/cctc.201700162>
- [13] A. Corma, M. Renz, Sn-Beta zeolite as diastereoselective water-resistant heterogeneous Lewis-acid catalyst for carbon–carbon bond formation in the intramolecular carbonyl–ene reaction, *Chem. Commun.*, (2004) 550-551, <https://doi.org/10.1039/B313738D>
- [14] Z. Wang, L. Wang, Y. Jiang, M. Hunger, J. Huang, Cooperativity of Brønsted and Lewis acid sites on zeolite for glycerol dehydration, *ACS Cat.*, 4 (2014) 1144-1147, <https://doi.org/10.1021/cs401225k>
- [15] A. Corma, M.E. Domine, L. Nemeth, S. Valencia, Al-free Sn-beta zeolite as a catalyst for the selective reduction of carbonyl compounds (Meerwein–Ponndorf–Verley reaction), *J. Am. Chem. Soc.*, 124 (2002) 3194-3195, <https://doi.org/10.1021/ja012297m>

- [16] Y. Zhu, G.-K. Chuah, S. Jaenicke, Selective Meerwein–Ponndorf–Verley reduction of  $\alpha,\beta$ -unsaturated aldehydes over Zr-zeolite beta, *J. Catal.*, 241 (2006) 25-33, <https://doi.org/10.1016/j.jcat.2006.04.008>
- [17] T.B. Boit, M.M. Mehta, N.K. Garg, Base-mediated Meerwein–Ponndorf–Verley reduction of aromatic and heterocyclic ketones, *Org. Lett.*, 21 (2019) 6447-6451, <https://doi.org/10.1021/acs.orglett.9b02342>
- [18] A. Corma, M.E. Domine, S. Valencia, Water-resistant solid Lewis acid catalysts: Meerwein–Ponndorf–Verley and Oppenauer reactions catalyzed by tin-beta zeolite, *J. Catal.*, 215 (2003) 294-304, [https://doi.org/10.1016/S0021-9517\(03\)00014-9](https://doi.org/10.1016/S0021-9517(03)00014-9)
- [19] J.F. Miñambres, J. Čejka, Meerwein-Ponndorf-Verley reduction in current heterogeneous catalysis research: a review, *Catal. Rev.*, 66 (2024) 2111-2152, <https://doi.org/10.1080/01614940.2023.2197716>
- [20] J. Magano, J.R. Dunetz, Large-scale carbonyl reductions in the pharmaceutical industry, *Org. Process Res. Dev.*, 16 (2012) 1156-1184, <https://doi.org/10.1021/op2003826>
- [21] D.S.S. Jorqueira, L.F. de Lima, S.F. Moya, L. Vilcocoq, D. Richard, M.A. Fraga, R.S. Suppino, Critical review of furfural and furfuryl alcohol production: Past, present, and future on heterogeneous catalysis, *Appl. Catal. A-Gen.*, 665 (2023) 119360, <https://doi.org/10.1016/j.apcata.2023.119360>
- [22] H. Li, J. He, A. Riisager, S. Saravanamurugan, B. Song, S. Yang, Acid–base bifunctional zirconium N-Alkyltriphosphate nanohybrid for hydrogen transfer of biomass-derived carboxides, *ACS Cat.*, 6 (2016) 7722-7727, <https://doi.org/10.1021/acscatal.6b02431>
- [23] O. Bortnovsky, Z. Sobalík, B. Wichterlová, Z. Bastl, Structure of Al–Lewis site in beta zeolite active in the Meerwein–Ponndorf–Verley reduction of ketone to alcohol, *J. Catal.*, 210 (2002) 171-182, <https://doi.org/10.1006/jcat.2002.3661>
- [24] A.A. Wismeijer, A.P.G. Kieboom, H. Van Bekkum, Selective hydrogenation of citronellal to citronellol over Ru/TiO<sub>2</sub> as compared to Ru/SiO<sub>2</sub>, *Appl. Catal.*, 25 (1986) 181-189, [https://doi.org/10.1016/S0166-9834\(00\)81235-X](https://doi.org/10.1016/S0166-9834(00)81235-X)
- [25] M. Boronat, A. Corma, M. Renz, Mechanism of the Meerwein–Ponndorf–Verley–Oppenauer (MPVO) Redox Equilibrium on Sn– and Zr–Beta Zeolite Catalysts, *J. Phys. Chem. B*, 110 (2006) 21168-21174, <https://doi.org/10.1021/jp063249x>
- [26] J.C. van der Waal, E.J. Creighton, P.J. Kunkeler, K. Tan, H. van Bekkum, Beta–type zeolites as selective and regenerable catalysts in the Meerwein–Ponndorf–Verley reduction of carbonyl compounds, *Top. Catal.*, 4 (1997) 261-268, <https://doi.org/10.1023/A:1019160827175>
- [27] M. Boronat, A. Corma, M. Renz, P.M. Viruela, Predicting the Activity of Single Isolated Lewis Acid Sites in Solid Catalysts, *Chem. Eur. J.*, 12 (2006) 7067-7077, <https://doi.org/10.1002/chem.200600478>
- [28] V. Montes, J.F. Miñambres, A.N. Khalilov, M. Boutonnet, J.M. Marinas, F.J. Urbano, A.M. Maharramov, A. Marinas, Chemoselective hydrogenation of furfural to furfuryl alcohol on ZrO<sub>2</sub> systems synthesized through the microemulsion method, *Catal. Today*, 306 (2018) 89-95, <https://doi.org/10.1016/j.cattod.2017.05.022>
- [29] K. Gołabek, S. Kurucová, J.F. Miñambres, K. Veselá, T. Zakeri, J. Přeck, Zr-site Lewis acidity determines terpenoid reduction selectivity, *ACS Catal.* 16 (2026) 3307-3318. <https://doi.org/10.1021/acscatal.5c07220>
- [30] V.L. Sushkevich, A. Vimont, A. Travert, I.I. Ivanova, Spectroscopic Evidence for Open and Closed Lewis Acid Sites in ZrBEA Zeolites, *J. Phys. Chem. C*, 119 (2015) 17633-17639, <https://doi.org/10.1021/acs.jpcc.5b02745>



- [31] J.A. Vannucci, M.S. Legnoverde, B.O. Dalla Costa, E.I. Basaldella, N.N. Nichio, F. Pompeo, Al-free Zr-beta zeolite as a selective catalyst for the ketalization of glycerol, *Mol. Catal.*, 528 (2022) 112497, <https://doi.org/10.1016/j.mcat.2022.112497>
- [32] J.W. Harris, M.J. Cordon, J.R. Di Iorio, J.C. Vega-Vila, F.H. Ribeiro, R. Gounder, Titration and quantification of open and closed Lewis acid sites in Sn-Beta zeolites that catalyze glucose isomerization, *J. Catal.*, 335 (2016) 141-154, <http://dx.doi.org/10.1016/j.jcat.2015.12.024>
- [33] G. Yang, L. Zhou, X. Han, Lewis and Brönsted acidic sites in M4+-doped zeolites (M=Ti, Zr, Ge, Sn, Pb) as well as interactions with probe molecules: A DFT study, *J. Mol. Catal. A-Chem.*, 363-364 (2012) 371-379, <https://doi.org/10.1016/j.molcata.2012.07.013>
- [34] P. Mäki-Arvela, N. Kumar, V. Nieminen, R. Sjöholm, T. Salmi, D.Y. Murzin, Cyclization of citronellal over zeolites and mesoporous materials for production of isopulegol, *J. Catal.*, 225 (2004) 155-169, <https://doi.org/10.1016/j.jcat.2004.03.043>
- [35] H. Zhang, Z.J. Quek, S. Jaenicke, G.-K. Chuah, Hydrophobicity and co-solvent effects on Meerwein-Ponndorf-Verley reduction/dehydration cascade reactions over Zr-zeolite catalysts, *J. Catal.*, 400 (2021) 50-61, <https://doi.org/10.1016/j.jcat.2021.05.011>
- [36] W. Li, S. Liu, H. Wang, B. Gao, C. Tu, Y. Luo, La-doped Zr-beta zeolite as efficient catalyst for reduction of cyclohexanone to cyclohexanol via the MPV process, *Catalysis Communications*, 133 (2020) 105845, <https://doi.org/10.1016/j.catcom.2019.105845>
- [37] J. Shabtai, R. Lazar, E. Biron, Catalysis of organic reactions by molecular sieve systems: 1. Meerwein-Ponndorf-Verley reductions, *J. Mol. Catal. A*, 27 (1984) 35-43, [https://doi.org/10.1016/0304-5102\(84\)85068-3](https://doi.org/10.1016/0304-5102(84)85068-3)
- [38] R. Bermejo-Deval, M. Orazov, R. Gounder, S.-J. Hwang, M.E. Davis, Active Sites in Sn-Beta for Glucose Isomerization to Fructose and Epimerization to Mannose, *ACS Catal.*, 4 (2014) 2288-2297, 10.1021/cs500466j
- [39] R. Otomo, R. Kosugi, Y. Kamiya, T. Tatsumi, T. Yokoi, Modification of Sn-Beta zeolite: characterization of acidic/basic properties and catalytic performance in Baeyer–Villiger oxidation, *Catal. Sci. Technol.*, 6 (2016) 2787-2795, <https://doi.org/10.1039/C6CY00532B>
- [40] L. Gao, G. Li, Z. Sheng, Y. Tang, Y. Zhang, Alkali-metal-ions promoted Zr-Al-Beta zeolite with high selectivity and resistance to coking in the conversion of furfural toward furfural alcohol, *J. Catal.*, 389 (2020) 623-630, <https://doi.org/10.1016/j.jcat.2020.07.002>
- [41] Database of Zeolite Structures, IZA-SC (International Zeolite Association Structure Commission), 2025.
- [42] R. Shannon, Revised effective ionic radii and systematic studies of interatomic distances in halides and chalcogenides, *Acta Crystallogr. A*, 32 (1976) 751-767, <https://doi.org/10.1107/S0567739476001551>
- [43] L. Kubelková, J. Čejka, J. Nováková, Surface reactivity of ZSM-5 zeolites in interaction with ketones at ambient temperature (a FT-i.r. study), *Zeolites*, 11 (1991) 48-53, [https://doi.org/10.1016/0144-2449\(91\)80355-4](https://doi.org/10.1016/0144-2449(91)80355-4)
- [44] S. Roy, K. Bakhmutsky, E. Mahmoud, R.F. Lobo, R.J. Gorte, Probing Lewis Acid Sites in Sn-Beta Zeolite, *ACS Catal.*, 3 (2013) 573-580, <https://doi.org/10.1021/cs300599z>
- [45] A.G. Pelmenschikov, R.A. van Santen, J. Janchen, E. Meijer, Acetonitrile-d<sub>3</sub> as a probe of Lewis and Brönsted acidity of zeolites, *J. Phys. Chem.*, 97 (1993) 11071-11074, <https://doi.org/10.1021/j100144a028>
- [46] B.A. Johnson, J.R. Di Iorio, Y. Román-Leshkov, Identification and quantification of distinct active sites in Hf-Beta zeolites for transfer hydrogenation catalysis, *J. Catal.*, 404 (2021) 607-619,

<https://doi.org/10.1016/j.jcat.2021.10.026>

- [47] M. Shamzhy, B. Gil, Acidity of Zeolites, in: D.P. Serrano, J. Čejka (Eds.) Zeolites: From Fundamentals to Emerging Applications, Royal Society of Chemistry, Cambridge, 2025, pp. 197-231.
- [48] J. Clayden, N. Greeves, S. Warren, Organic Chemistry, Oxford University Press, New York, 2012.
- [49] K.H. Møller, A. Kjaersgaard, A.S. Hansen, L. Du, H.G. Kjaergaard, Hybridization of nitrogen determines hydrogen-bond acceptor strength: gas-phase comparison of redshifts and equilibrium constants, J. Phys. Chem. A, 122 (2018) 3899-3908, <https://doi.org/10.1021/acs.jpca.8b00541>
- [50] E.P.L. Hunter, S.G. Lias, Evaluated gas phase basicities and proton affinities of molecules: an update, J. Phys. Chem. Ref. Data, 27 (1998) 413-656, <https://doi.org/10.1063/1.556018>
- [51] Acetone, in: NIST Standard Reference Database Number 69, National Institute of Standards and Technology, 2025, DOI: <https://doi.org/10.18434/T4D303>
- [52] N. Abidi, Y. Boudjema, C. Chizallet, K. Larmier, Investigating closed and open site stability of Sn-, Ti-, Zr-, and Hf-beta zeolites: a comprehensive periodic DFT study, J. Phys. Chem. C, 128 (2024) 8257-8269, <https://doi.org/10.1021/acs.jpcc.4c02371>